



HAL
open science

Multiuser Chirp Spread Spectrum Transmission in an Underwater Acoustic Channel Applied to an AUV Fleet

Christophe Bernard, Pierre-Jean Bouvet, Antony Pottier, Philippe Forjonel

► **To cite this version:**

Christophe Bernard, Pierre-Jean Bouvet, Antony Pottier, Philippe Forjonel. Multiuser Chirp Spread Spectrum Transmission in an Underwater Acoustic Channel Applied to an AUV Fleet. *Sensors*, 2020, 20 (5), pp.1527. 10.3390/s20051527. hal-02903378

HAL Id: hal-02903378

<https://hal.science/hal-02903378>





Submitted on 21 Jul 2020

HAL is a multi-disciplinary open access archive for the deposit and dissemination of scientific research documents, whether they are published or not. The documents may come from teaching and research institutions in France or abroad, or from public or private research centers.

L'archive ouverte pluridisciplinaire **HAL**, est destinée au dépôt et à la diffusion de documents scientifiques de niveau recherche, publiés ou non, émanant des établissements d'enseignement et de recherche français ou étrangers, des laboratoires publics ou privés.

Article

Multiuser chirp spread spectrum transmission in an underwater acoustic channel applied to an AUV fleet

 Christophe Bernard ¹,  Pierre-Jean Bouvet^{1,*},  Antony Pottier ¹ and  Philippe Forjonel¹

¹ L@bISEN - Yncréa Ouest; ISEN Brest; firstname.lastname@isen-ouest.yncrea.fr

* Author to whom correspondence should be addressed.

Academic Editor: name

Version March 3, 2020 submitted to Sensors

Abstract: The objective of this paper is to provide a multiuser transmission technique for underwater acoustic communication in the framework of Autonomous Underwater Vehicle (AUV) fleet. By using a variant of an Hyperbolically Frequency Modulated (HFM) signal, we describe a new family of transmission techniques called MultiUser Chirp Spread Spectrum (MU-CSS) that allows a very simple matched filter based decoding. These techniques are expected to provide good resilience against multiuser interference while keeping good robustness to the Underwater Acoustic (UWA) channel impairments like Doppler shift. Their implementation for the UWA scenario are described, and performance results over a simulated shallow water UWA channel are analysed and compared against the conventional Code-Division Multiple Access (CDMA) and Time-Division Multiple Access (TDMA) transmission. Finally, feasibility and robustness of the proposed methods are verified over the underWater AcousTic channEl Replay benchMARK (Watermark) fed by several channel responses from sounding experiments performed in a lake.

Keywords: Underwater communications; multiple access; chirp spread spectrum; direct sequence spread spectrum; code division multiple access (CDMA); time division multiple access (TDMA).

1. Introduction

The UWA channel is one of the most challenging channels for data communications. Due to the low celerity of acoustic waves ($c = 1500 \text{ m.s}^{-1}$), UWA channels are characterized by extensive multipath effects and large Doppler spreads. Moreover frequency dependent attenuation, temporal variations and background noise limit the achievable data rate considerably [1][2]. On the other hand, AUVs are used for several marine applications such as in military field with anti-submarine warfare, science field with wreck exploration, or in industrial field with offshore energy research. Nowadays the concept of several AUVs working together within a fleet is an on-going research axis [3]. UWA communication with an AUV fleet is used to control vehicles (downlink) or to gather data from vehicles (uplink). The quality and reliability of communications is essential, mainly in shallow water areas for which the multipath effect is stronger, leading to extensive intersymbol interference.

Multiuser communication protocols in an UWA channel can be divided into two categories, random or deterministic protocols. In random protocols, data rate cannot be predicted in advance due to the phenomenon of collisions between different users. A classical examples of random protocol is ALOHA [4] and its variants [5] which use the long propagation delays to reduce the number of collisions and consequently to increase the data rate. An other example of random protocol is the Carrier Sense Multiple Access (CSMA) method [6] which is based on channel listening to avoid collisions. On the other side, deterministic protocols perform deterministic assignments of channel resources to the users so that their activity on the channel is predictable. The method we propose in

35 this paper aims at building a new set of mutually orthogonal waveforms to be assigned to the users
 36 of an UWA channel, so as to separate them easily at the receiver side. This falls consequently in the
 37 class of deterministic protocols. Traditional methods for deterministic, multiuser, UWA transmissions
 38 are inspired by radio communications and adapted to the UWA channel. As examples, we can
 39 cite the TDMA [7], Frequency Division Multiple Access (FDMA) [8], CDMA [9] and Multi-Carrier
 40 Code-Division Multiple Access (MC-CDMA) [10] transmissions. Typically, FDMA is considered
 41 inefficient since UWA channel has limited bandwidth and exhibits large Doppler spread that requires
 42 guard frequency bands between users leading to data rate wasting. MC-CDMA transmission schemes
 43 suffer from both time/frequency selectivity of UWA channel and multiple-access interference, and
 44 require complex iterative equalizers. Consequently, in the following we will focus only on TDMA and
 45 CDMA multiple access strategies. TDMA allows several users to share the same frequency channel by
 46 dividing the signal into different time slots. Each user uses alternatively its own time slot to transmit
 47 data without interfering with other users. However, as the number of users increases, the waiting
 48 time per user increases and the user data rate decreases. In CDMA transmission, the different users
 49 transmit information data simultaneously through a different spreading sequence for each user. The
 50 disadvantage of this method lies in the multiuser interference provided by the non-orthogonality
 51 of spreading sequences especially when the user communication channel is selective in time or in
 52 frequency. Moreover such effect is increased when the interference power is much larger than the
 53 received signal power. This phenomenon is well known in mobile communication networks as the
 54 *near-far* problem. To cope with interference terms in CDMA, advanced equalization schemes can be
 55 invoked, such as multiuser detection [11] or Multi-User Multiple-Input Multiple-Output (MU-MIMO)
 56 technique combined with Passive Phase Conjugation (PPC) [12], but at the prize of a higher decoding
 57 complexity and a limited number of users. Recently, the authors of [13] proposed an alternative of
 58 CDMA and TDMA by using chirp waveforms for UWA multiuser communication. To reduce the
 59 multiuser interference, the Virtual Time Reversal Mirror (VTRM) technique is used with a Fractional
 60 Fourier Transform (FrFT) at the reception. However, this method requires an estimate of the different
 61 channels and is limited to 4 users because of interference.

62
 63 In this paper, we describe a new transmission scheme based on Chirp Spread Spectrum (CSS)
 64 entitled MU-CSS that we originally introduced in [14]. The basic idea consists in building a set of
 65 mutually orthogonal chirp-based waveforms which will be resistant to Doppler spread and Doppler
 66 shift. The objective is on the one hand to take benefit from the robustness of chirps against UWA
 67 channel impairments and, on the other hand, to use orthogonality to separate multiple users at the
 68 receiver side, using a simple matched filter. With respect to [14], we derive three new methods to build
 69 MU-CSS that optimize mutual orthogonality between waveforms. By assuming an uplink scenario
 70 where a fleet of N_u AUVs in motion needs to transmit data to a receiver situated at the sea surface,
 71 we provide performance comparison of each method over simulated and experimental replay channels.

72
 73 The paper is organized as follows: System model and state of the art of multiuser transmissions
 74 are introduced in Section 2. The proposed MU-CSS multiuser schemes are presented in Section 3.
 75 Performance results of the proposed schemes against conventional multiuser transmissions are carried
 76 out in Section 4 by using shallow water UWA channel simulator derived from [15,16] and in Section 5
 77 by using Watermark replay channel [17] fed by experiments conducted in Ty-Colo lake, Saint-Renan,
 78 France. Finally, conclusions are drawn in Section 6.

79
 80 In the following, $\|\cdot\|_2$ denotes the euclidean norm, $\langle \cdot \rangle$ the scalar product, $\mathbb{E}\{\cdot\}$ denotes the
 81 statistical expectation, $(\cdot)^*$ the complex conjugate and $u * v$ denotes the convolution product between
 82 u and v .

83 2. Multiuser transmission

84 2.1. System model

85 2.1.1. Transmitted signal

86 Let $d_{i,k}$ be the k -th symbol transmitted by the i -th user, we assume that $d_{i,k}$ belong to a
87 unit-amplitude Phase Shift Keying (PSK) alphabet, and are differentially encoded such that:

$$d_{i,k} = d_{i,k-1} \cdot b_{i,k} \quad \text{with } i \in [1, N_u], k \in [2, N_s] \quad (1)$$

88 where b_k is the original PSK data symbol, and $d_{i,0}$ is set to 1. Beforehand, the data symbols $b_{i,k}$
89 are protected by a Forward Error Correction (FEC) code followed by a random interleaver. In the
90 following, the FEC code type will be an half-rate convolutional code with code generator (133, 171)_o.
91 Moreover, N_u denotes the number of users and N_s the number of data symbols per frame. The choice
92 of Differential Phase Shift Keying (DPSK) is motivated by the rapid fluctuation of UWA channel and
93 thus allows to avoid the use of channel equalizers at the receiver side, which are sensitive to outdated
94 channel estimations [18]. Thus, in a UWA communication channel with large delay spreads and rapid
95 time variations, differential modulation are demonstrated to provide interesting performance and
96 even outperform coherent modulation under certain conditions [19].

97
98 Let $g_i(t)$ the transmit waveform associated to user i and T_s the symbol duration, the baseband
99 transmit signal for user i can be written as:

$$s_i(t) = \sum_{k=1}^{N_s} d_{i,k} g_i(t - kT_s) \quad (2)$$

100 2.2. Underwater multiuser channel

101 By assuming that users are mobile with relative motion v_i , positive values of v_i denote motion
102 away from the receiver, while negative values denote motion toward the receiver, the received baseband
103 signal is given by:

$$r(t) = \sum_{i=1}^{N_u} \int_{-\infty}^{+\infty} h_i(\tau, t) s_i((1 - a_i)(t - \tau)) e^{j2\pi f_c a_i (t - \tau)} d\tau + n(t) \quad (3)$$

104 with f_c the carrier frequency and $a_i = \frac{v_i}{c}$ the Doppler scale factor. The UWA channel impulse response
105 for the i -th user at time t is denoted by $h_i(\tau, t)$ and $n(t)$ represents the additive noise assumed
106 Gaussian and zero-mean.

108 2.2.1. User decoding

109 When the Doppler shift can be estimated at the receiver, the Doppler effect is usually removed
110 prior to decoding by resampling the received baseband signal and compensating phase rotation as
111 follows [1]:

$$z_i(t) = r \left(\frac{t}{1 - a_i} \right) e^{-j2\pi f_c \left(\frac{a_i}{1 - a_i} \right) t} \quad (4)$$

112 By assuming perfect time synchronization, information data of the i -th user can be estimated by
113 matched filtering $z_i(t)$ with the transmitted waveform of user i , followed by integration over a symbol
114 duration [20]:

$$\hat{d}_{i,k} = \max_{k\frac{T_s}{2} \leq t \leq (k+1)\frac{T_s}{2}} \left[\int_{-\infty}^{+\infty} g_i^*(-u) z_i(t-u) du \right] \quad (5)$$

$$= \int_{-\frac{T_s}{2}}^{\frac{T_s}{2}} g_i^*(t) z_i(t + kT_s) dt \quad (6)$$

$$= \gamma_{i,k} \hat{d}_{i,k} + \eta_{i,k} + w_{i,k} \quad (7)$$

115 where $\gamma_{i,k}$ denotes the bias of the decoder, $\eta_{i,k}$ the multiuser interference terms and $w_{i,k}$ the additive
116 noise terms, exact expression of these three terms is provided in the appendix A.

117 2.3. Conventional multiuser transmission schemes

118 2.3.1. CDMA

119 The objective of CDMA is to break up a finite transmission spectrum so that multiple users can
120 access it at the same time. To accomplish time multiplexing, a code, chosen in a set of mutually
121 orthogonal spreading codes, is assigned to each user [21]. For the i -th user, the transmitted waveform
122 is expressed by:

$$g_i(t) = c_i(t) = \sum_{l=0}^{N_{SF}-1} c_{i,l} \phi(t - lT_c) \quad (8)$$

123 with $[c_{i,1}, c_{i,2}, \dots, c_{i,N_{SF}}]$ the spreading code of length N_{SF} , T_c the chip duration, N_{SF} the spreading factor
124 and $\phi(t)$ the pulse shaping filter chosen as a Square Root Raised Cosine (SRRC) filter [20]. Since,
125 we are in an uplink scenario, CDMA system is asynchronous, and spreading codes are chosen as
126 Pseudo-Noise (PN) sequences generated pseudo-randomly such that their autocorrelation functions
127 tend to Dirac functions as N_{SF} grows, so that the mutual cross-correlation tends to zero.

128 At the receiver side, if $T_s > \tau_{max}$ where τ_{max} denotes the Root Mean Square (RMS) channel delay
129 spread, and if the communication channel is constant over a symbol duration T_s , the autocorrelation
130 properties and quasi-orthogonality between users of PN codes leads the term $\eta_{i,k}$ in (7) to become
131 negligible compared to $\gamma_{i,k}$ and thus allow to decode each user separately [20].
132

133 2.3.2. TDMA

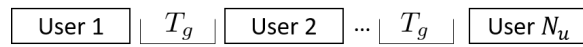


Figure 1. Scheme of TDMA.

134 In a TDMA approach, the users are time-multiplexed as depicted in Fig. 1. The time slot assigned
135 to one user is made of a frame slot of $N_s T_s$ seconds followed by a guard interval of duration T_g so
136 as to absorb multiuser interference. In order to deal with frequency selectivity of the UWA channel,
137 Direct Sequence Spread Spectrum (DSSS) signalling with the same modulation parameters as CDMA
138 is chosen for each user such that TDMA and CDMA approaches are equivalent in the single user
139 scenario. The baseband received signal and the decoding process are given by particularizing (2)
140 and (8) respectively with $N_u = 1$. One can note that more spectral efficient transmission scheme
141 could be chosen for TDMA (see [22] for example) but at the price of higher complexity at the receive
142 side. Moreover, higher spectral efficiency signaling scheme would make difficult the comparison with
143 CDMA especially in the single user case.

144 3. MU-CSS scheme

145 3.1. Generalities

146 By the use of frequency swept signals, which are resilient to the detrimental effects of the
 147 UWA channel, the CSS modulation technique offers robust performance with a very simple matched
 148 filtering-based decoder that makes such a communication scheme particularly adapted to the UWA
 149 communication channel [23,24]. In the CSS system, a broad spectrum is occupied to modulate the
 150 information in order to achieve high processing gain and multipath resolution to the detriment of the
 151 spectral efficiency. In the following, we construct 3 multiuser schemes based on CSS signaling and
 152 more precisely on HFM signal given by:

$$x(t) = \begin{cases} \cos(-2\pi(k \log(1 - \frac{t}{t_0}) + \frac{f_l + f_h}{2})) & \text{if } -\frac{T_s}{2} \leq t \leq \frac{T_s}{2} \\ 0 & \text{otherwise} \end{cases} \quad (9)$$

153 with $t_0 = \frac{T_s(f_h + f_l)}{2(f_h - f_l)}$, $k = \frac{T_s f_l f_h}{f_h - f_l}$, $f_l \leq f_h$ and T_s the duration of the HFM signal, whose instantaneous
 154 frequency is provided in figure 2 with $f_h = B/2$ and $f_l = -B/2$ where $B = 4$ kHz and $T_s = 7.75, 15.75,$
 155 31.75 ms.

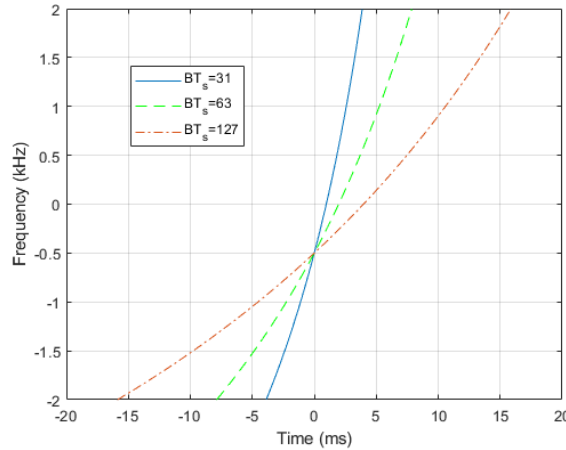


Figure 2. Instantaneous frequency of HFM waveform with $BT_s = 31, 63, 127$.

156 The basic idea of MU-CSS consists in building an orthogonal basis of signals $e_i(t)$ thanks to the
 157 Gram-Schmidt process where the waveform $e_i(t)$ is assigned to i -th user with $i \in [1, N_u]$. The initial
 158 orthogonality between waveforms is brought by the combination of the HFM signals with orthogonal
 159 spreading sequences that are chosen as a Walsh-Hadamard codes [21]. The set of spreading codes
 160 allows users to be differentiated at the receiver side while HFM waveform provides robustness against
 161 Doppler and delay spreads.
 162

163 3.2. MU-CSS Gram-Schmidt iterated

164 In this method, an iterative process is used to improve the mutual orthogonality between the
 165 chirp waveforms, as well as the immunity against channel impairments.

166 Let $e_i^{(l)}(t)$ denotes the waveform corresponding to the i -th user with $i \in \{1, 2, \dots, N_u\}$ at iteration
 167 $l \in \{1, N_{IT}\}$. The process is based on the Gram-Schmidt method [25], as follows, for $i > 0$:

$$e_i^{(l)}(t) = c_i(t) + \alpha_i^{(l)} e_{i-1}^{(l)}(t) \quad (10)$$

169 where:

$$\alpha_i^{(l)} = -\frac{\langle c_i(t), e_{i-1}^{(l)}(t) \rangle}{\|e_{i-1}^{(l)}(t)\|_2^2} = -\frac{\int_{-\frac{T_s}{2}}^{\frac{T_s}{2}} c_i(t) e_{i-1}^{(l)*}(t) dt}{\|e_{i-1}^{(l)}(t)\|_2^2} \quad (11)$$

170 with $c_i(t)$ given by equation (8). At the first iteration, we set $e_0^{(1)}(t) = x(t)$ where $x(t)$ is defined in (9)
171 and for $l > 1, i > 0$:

$$c_i(t) = e_i^{(l-1)}(t) \quad (12)$$

172 The final waveform assigned to each user is obtained after N_{IT} iterations of the above mentioned
173 process by setting $g_i(t) = e_i^{(N_{IT})}(t)$. The orthogonality between the different $e_i^{(l)}(t)$ and the choice for
174 the value of $\alpha_i^{(l)}$ are justified in the appendix B, using the Gram-Schmidt procedure.

175

176 3.3. MU-CSS Gram-Schmidt multiplication

177 In this method, the combination with the HFM is made by multiplying it with the spreading
178 sequence, while applying the Gram-Schmidt iteration process to ensure orthogonality. We start from:

$$e_i(t) = c_i(t) + \alpha_i e_{i-1}(t) \quad \text{with } i \in [1, N_u]. \quad (13)$$

179 with α_i defined in (11). Then we build:

$$\tilde{e}_i(t) = \bar{e}_i(t) + \beta_i \tilde{e}_{i-1}(t) \quad (14)$$

180 where $\bar{e}_0(t) = \tilde{e}_0(t) = x(t)$ (this signal will be excluded from the set later) and for $i > 0$:

$$\bar{e}_i(t) = x(t) e_i(t) \quad (15)$$

181 Moreover:

$$\beta_i = -\frac{\langle \bar{e}_i(t), \tilde{e}_{i-1}(t) \rangle}{\|\tilde{e}_{i-1}(t)\|_2^2} = -\frac{\int_{-\frac{T_s}{2}}^{\frac{T_s}{2}} \bar{e}_i(t) \tilde{e}_{i-1}^*(t) dt}{\|\tilde{e}_{i-1}(t)\|_2^2} \quad (16)$$

182 The final waveform assigned to each user is obtained by setting $g_i(t) = \tilde{e}_i(t)$.

183 3.4. MU-CSS Gram-Schmidt insertion

184 In this last variant, we combine the previous method with the insertion of an HFM signal at
185 regular intervals such as:

$$\tilde{e}_i(t) = \begin{cases} x(t) & \text{if } i = kp \text{ with } k \in \mathbb{N}^* \\ x(t) e_i(t) & \text{else} \end{cases} \quad (17)$$

186 with p the insertion step. The idea is to try to improve the robustness of the different waveforms. To
187 impose orthogonality between spread signals, we simply apply equations (13) and (14) and finally get
188 $g_i(t) = \tilde{e}_i(t)$.

189 4. Simulation results

190 4.1. Underwater acoustic channel simulator

191 For the simulation comparisons, we consider the UWA channel simulator provided by [15] based
 192 on a stochastic model. The time-varying transfer function for the i -th user is given by:

$$H_i(f, t) = \bar{H}_i(f) \sum_p h_{i,p} \gamma_{i,p}(f, t) e^{-j2\pi f \tau_{i,p}(t)} \quad (18)$$

193 with $\bar{H}_i(f)$ the transfer function of direct path, $h_{i,p}$ the relative path gain, $\gamma_{i,p}(f, t)$ represents the
 194 scattering coefficient modeled by a complex-valued Gaussian processes whose statistics reflects the
 195 time coherence of the channel, and $\tau_{i,p}(t)$ denotes time-varying delay of the p -th path and can be
 196 expressed as:

$$\tau_{i,p}(t) = \bar{\tau}_{i,p} - (\bar{a}_i + a_{i,p})t \quad (19)$$

197 where $\bar{\tau}_{i,p}$ is the average delay of path p and \bar{a}_i represents the mean Doppler shift induced by the
 198 motion of i -th AUV relatively to the receiver. In the following we will assume that \bar{a}_i is known at the
 199 receiver side and compensated. Moreover, $a_{i,p}$ is the residual Doppler factor that captures resulting
 200 motion-induced time scaling on the p -th path. Coefficients $a_{i,p}$ are assumed to be constant over a frame
 201 and to follow a zero-mean Gaussian distribution with variance σ_a^2 . Time variations of $\gamma_{i,p}(f, t)$ and
 202 $\tau_{i,p}(t)$ lead to Doppler spread effects [15].

203 4.2. System parameters

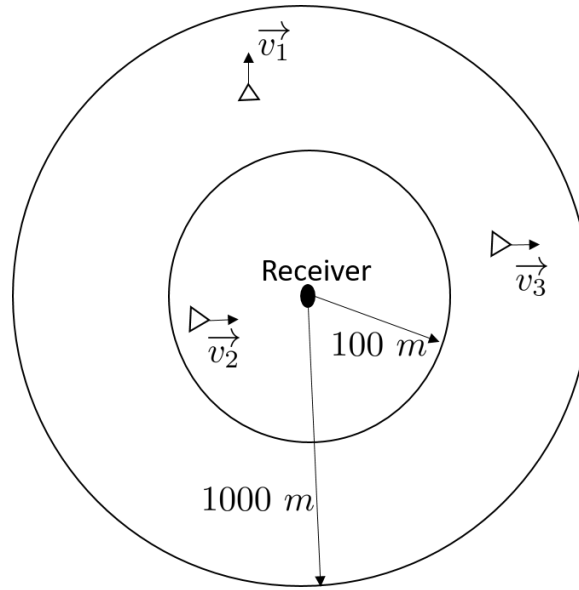


Figure 3. Scheme of the simulated system.

204 The chosen model represents a short range UWA transmission with a 10 m water depth at a center
 205 frequency of 23 kHz over a 4 kHz bandwidth. Each AUV are supposed at a same depth of 1 m. At the
 206 beginning of the simulations, the range between each AUV and the receiver is randomly selected in the
 207 interval $[0.1, 1]$ km modeling a fleet situating in a circular area (Fig. 3). Channel model parameters are
 208 summarized in Table 1 whereas transmission system parameters are provided in Table 2. The symbol
 209 duration is set according to the channel delay spread such that $T_s > \tau_{max}$ and is fixed identical for all

210 protocols. Evolution of simulated channel impulse response $|h_i(\tau, t)|$ over one frame is provided in
 211 figure 4.

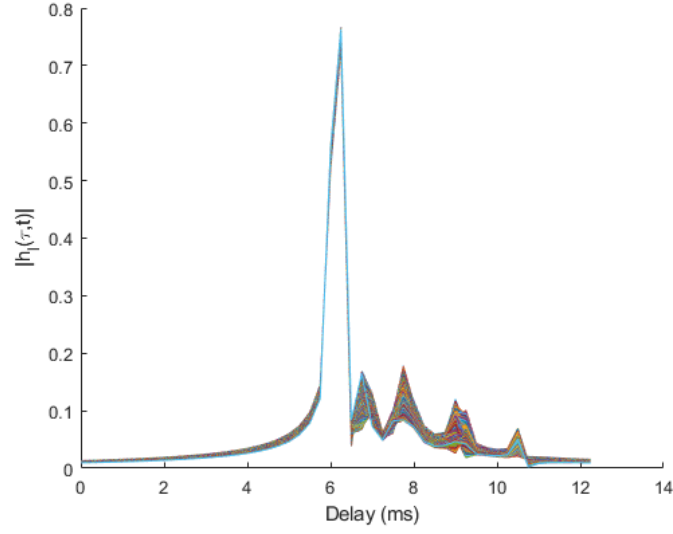


Figure 4. Evolution of the simulated time-varying channel impulse response over one frame based on the parameters provided in Table 1.

Table 1. UWA channel model parameters.

Symbol	Signification	Value
f_c	Center frequency	23 kHz
N_u	Number of AUVs	[1, 10]
f_s	Sample frequency	100 kHz
B	Signal bandwidth	4 kHz
D_i	Transmission range	[0.1, 1] km
z_w	Water depth	10 m
τ_{max}	RMS channel delay spread [20]	[0.52, 0.84] ms
SNR	Signal to noise ratio	10 dB
v_i	User relative speed	[-2, 2] m/s
σ_a	Residual motion-induced Doppler spread standard deviation	10^{-5}

212 4.3. Orthogonality verification

213 To verify the orthogonality of the proposed waveform, we compute the
 214 Signal-to-Interference-plus-Noise Ratio (SINR) obtained after matched filtering. Following
 215 (7), for user i , we have:

$$\text{SINR} = \frac{\mathbb{E}\left\{|\gamma_{i,k}|^2\right\}}{\mathbb{E}\left\{|\eta_{i,k}|^2\right\} + \mathbb{E}\left\{|w_k|^2\right\}} \quad (20)$$

216 Simplifying (A4), (A5) and (A8) in the case of static AUV motion (i.e. $a_i = 0$) and channel delay spread
 217 very small compared to the symbol duration (i.e. $T_s \gg \tau_{max}$), the last equation becomes:

$$\text{SINR} = \frac{\left| \int_{-\frac{T_s}{2}}^{\frac{T_s}{2}} g_i^*(t) \left(\int_{-\infty}^{+\infty} h_i(t, \tau) g_i(t - \tau) d\tau \right) dt \right|^2}{\left| \sum_{\substack{j=1 \\ j \neq i}}^{N_u} \int_{-\frac{T_s}{2}}^{\frac{T_s}{2}} g_i^*(t) \left(\int_{-\infty}^{+\infty} h_j(t, \tau) g_j(t - \tau) d\tau \right) dt \right|^2 + \mathbb{E}\left\{ \left| \int_{-\frac{T_s}{2}}^{\frac{T_s}{2}} g_i^*(t) n(t) dt \right|^2 \right\}} \quad (21)$$

Table 2. System parameters.

Symbol	Signification	Value
M	Modulation order	2 (DBPSK)
N_s	Number of symbols per frame	200
N_f	Number of frames	5000
\mathcal{C}	FEC code type	Convolutional code
g_C	FEC code generator	$(133, 171)_o$
R_C	FEC code rate	$\frac{1}{2}$
T_g	Guard interval time	15 ms
T_h	Duration of the chirp signal	7.75 ms
T_c	Chip duration	0.25 ms
N_{SF}	PN length code	31
N_{IT}	Number of iterations	1000
p	Insertion step	7
α	Pulse shaping filter roll-off factor	0.25
T_s	Symbol duration	7.75 ms

218 In figure 5, we compute numerically the SINR by using (21) and the system parameters depicted
 219 in table 2 over an Additive White Gaussian Noise (AWGN) channel and also over the time-varying
 220 UWA channel with static users described in Section 4.1. Comparisons are performed between MU-CSS,
 221 CDMA and TDMA transmissions. At $N_u = 1$ user, since there are no interference terms, all the
 222 transmission techniques have the same SINR after matched filter decoding, which is equal to channel
 223 Signal-to-Noise Ratio (SNR) added to the spreading gain in the case of AWGN channel. Naturally, as
 224 the the number of users increases, SINR decreases due to the growing importance of the interference
 225 terms, excepted for the TDMA case for which interference terms are absent whatever the number
 226 of users, thanks to time multiplexing. In both AWGN and UWA channels, MU-CSS transmissions
 227 outperform CDMA demonstrating that Gram-Schmidt based construction method provides good
 228 orthogonality properties for MU-CSS waveforms. This SINR gap is mainly explained by the use of
 229 PN sequences in CDMA that are not perfectly orthogonal (but only quasi-orthogonal) while MU-CSS
 230 employs waveforms that are orthogonal owing to the Gram-Schmidt process. Obviously, this SINR
 231 gap could be erased in AWGN by the use of orthogonal codes like Walsh-Hadamard sequences for
 232 CDMA, however such codes are not suitable in the uplink scenario.

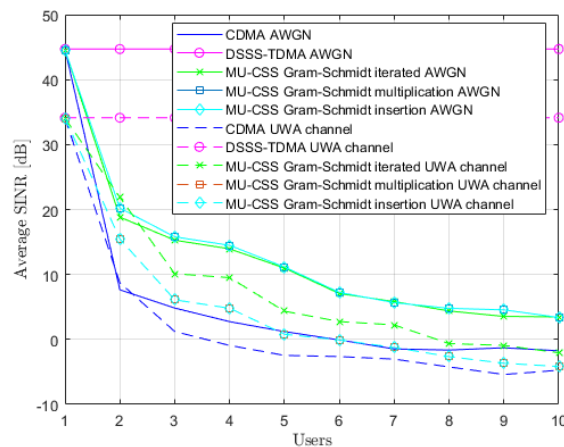


Figure 5. Average SINR for different waveforms over AWGN and time-varying UWA channel with static users, SNR = 30 dB.

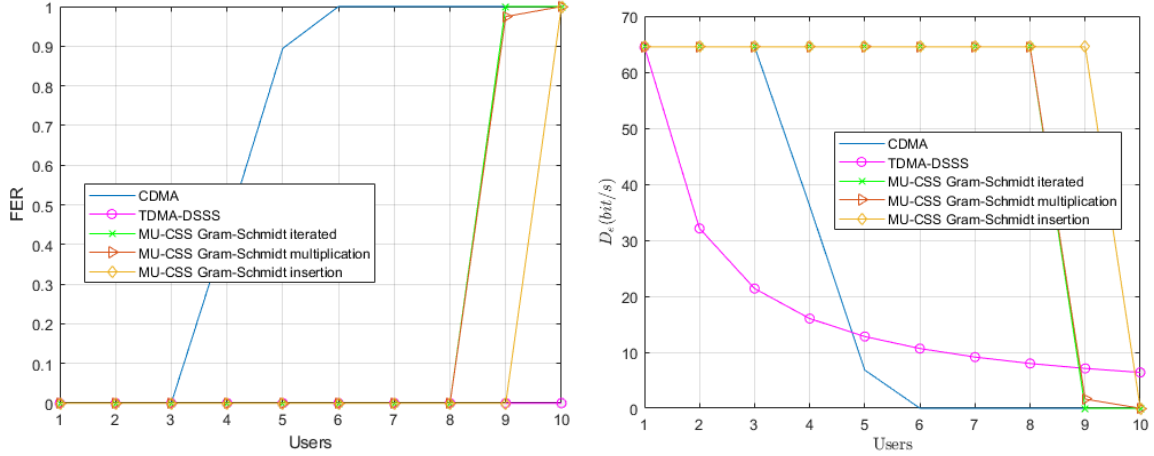


Figure 6. Average FER performance (left) and effective data rate (right) versus number of users over static simulated UWA channel model.

233 4.4. Performance metrics

234 As performance metrics, we consider the average effective data rate per user defined for each
 235 transmission technique as follows:

$$D_e^{\text{CDMA}} = \frac{R_C \log_2 M}{N_{SF} T_c} \cdot (1 - \text{FER}) \quad [\text{bps}] \quad (22)$$

$$D_e^{\text{TDMA}} = \frac{R_C \log_2 M}{N_u N_{SF} T_c + (N_u - 1) T_g} \cdot (1 - \text{FER}) \quad [\text{bps}] \quad (23)$$

$$D_e^{\text{MU-CSS}} = \frac{R_C \log_2 M}{T_h} \cdot (1 - \text{FER}) \quad [\text{bps}] \quad (24)$$

236 where M is the size of the DPSK constellation, R_C is channel coding rate and FER is the Frame Error
 237 Rate. A frame is considered erroneous when at least one bit per frame after channel decoding is
 238 erroneous.

239

240 4.5. Static channel

241 In a first step we consider a static UWA channel leading to only frequency selective fading.
 242 This yields constant parameters $\gamma_p(f, t)$ and $\tau_p(t)$ in time, in equation (18). Frame Error Rate (FER)
 243 performance and effective data rate of each transmission technique over the modeled shallow water
 244 acoustic channel are provided in Fig. 6.

245

246 In the single-user scenario, the 3 transmission techniques have a FER of 0 and as expected, the
 247 FER of TDMA remains unchanged when the number of users increases. Above 4 users, the interfering
 248 terms of the CDMA, expressed in equation (7) by the quantity $\eta_{i,k}$, make impossible the decoding of
 249 each user. On the other side, the largest number of users that can be handled by the MU-CSS is 8 or
 250 9 depending on the method. The fact that MU-CSS outperforms CDMA is mainly explained by the
 251 better orthogonality properties of the MU-CSS waveforms.

252

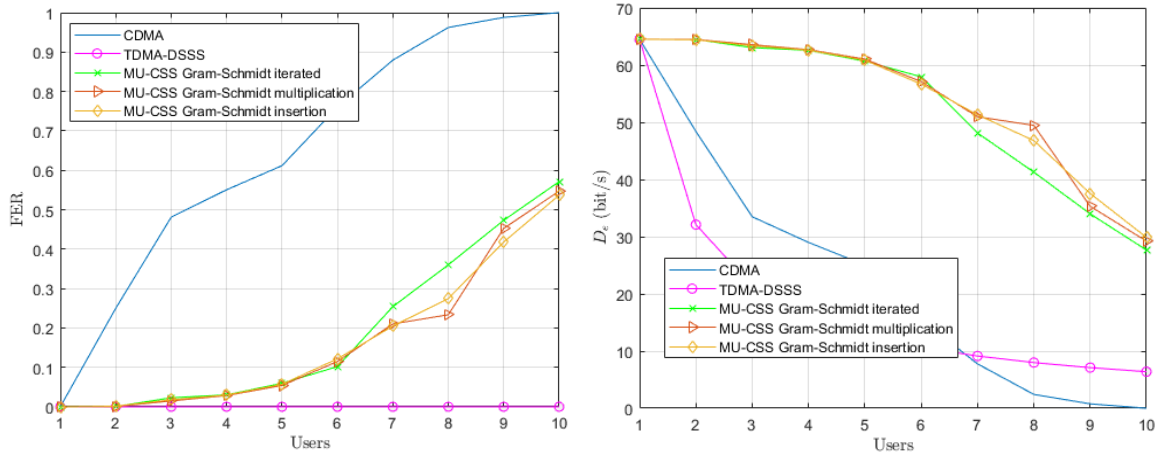


Figure 7. Average FER performance (left) and effective data rate (right) versus number of users over time-varying simulated UWA channel model with static users

253 4.6. Time varying channel and static users

254 In a second step, we consider a time-varying channel model where Doppler spread effect is
 255 provided in the equation (18) by $\gamma_i(f, t)$ and $\tau_{i,p}(t)$ coefficients. In this scenario, we assume that all
 256 users are static yielding to $\bar{a}_i = 0$ in relation (19). Performance over time varying channel with static
 257 users is depicted in Fig. 7.

258
 259 Doppler spread effect provided by multipath time-variations leads to an FER increase of both
 260 CDMA and MU-CSS transmissions, while TDMA decoding performance still remains error free. In
 261 fact, TDMA transmission is not affected by multiuser interference but only UWA channel time and
 262 frequency selectivity while CDMA and MU-CSS suffers from multiuser interference in addition to the
 263 UWA channel selectivity. The MU-CSS transmissions have the best effective data rate compared to
 264 CDMA because the HFM signal makes the spreading signals resistant against channel impairments
 265 such as Doppler spread. Among the MU-CSS transmission technique, the Gram-Schmidt iterated
 266 method appears to be slightly less robust than the other methods.

267 4.7. Time varying channel and mobile users

268 In a last step, we consider, a time varying channel model with mobile AUV whose speed is
 269 randomly selected in the interval $[-2, 2]$ m/s at each frame and for each user. The motion induced
 270 Doppler shift is assumed to be perfectly known and compensated at the reception for each user i .
 271 According to (4), since each user has different speed, Doppler compensation of user i will increase
 272 power of interference terms. However, in practice, Doppler shift is unknown and must be estimated
 273 prior to decoding [26].

274
 275 Performance over time-varying UWA channel with mobile users is carried out in Fig. 8. In
 276 the single-user scenario, the three transmission techniques provide an FER of 0% and, as expected,
 277 FER of TDMA remains unchanged when the number of users increases. Both CDMA and MU-CSS
 278 transmissions are severely impacted by motion-induced Doppler shift, since Doppler shift correction
 279 for an user also applies to other users according to equation (4). However MU-CSS transmissions still
 280 outperforms CDMA, which might be explained by the MU-CSS construction that provides both an
 281 orthogonality enhancement and a better robustness against Doppler shift. Beyond 6 users, the TDMA
 282 approach is more efficient in terms of data rate.

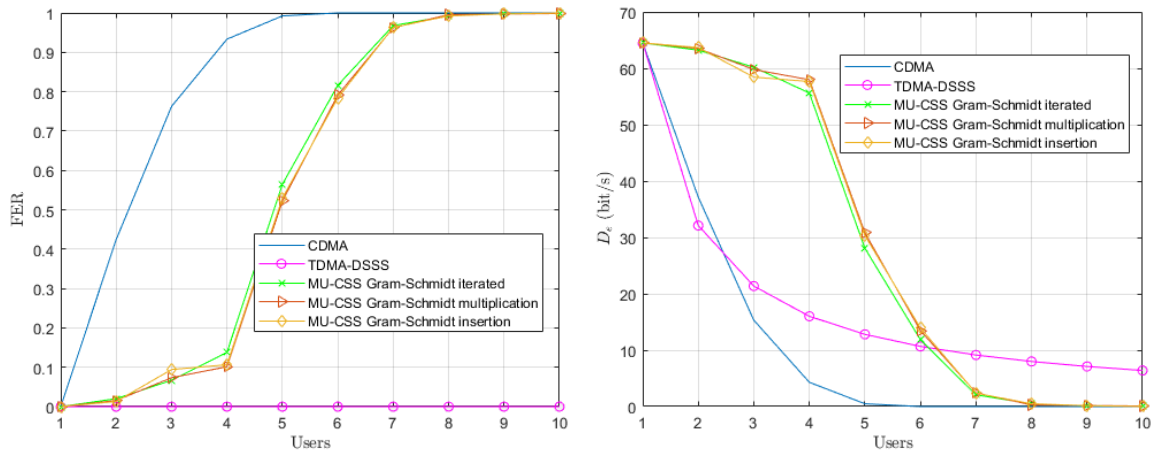


Figure 8. Average FER performance (left) and effective date rate (right) versus number of users over time varying UWA channel model with mobile users.

283 5. Experimental results

284 5.1. Channel sounding

285 5.1.1. Ty-Colo lake of Saint-Renan (France)

286 The sounding experiments took place in July 2019 at the lake of Ty-Colo, Saint Renan, France. The
 287 depth of the lake is around 5 m and up to 10 transmission ranges between [47, 364] m were sounded
 288 successively with one hydrophone at the receiver side as depicted in Fig. 9. Each channel sounding
 289 was performed during 3 min 30s, using a 255-Maximal Length Sequence (MLS) probe signal [27]
 290 centered on $f_c = 27$ kHz over a 6 kHz bandwidth. Fig. 10 provides an example of the delay-Doppler
 291 spread extracted from the successive estimated Channel Impulse Response (CIR). Estimated channel
 292 delay spreads and Doppler spreads are reported in Table 3.

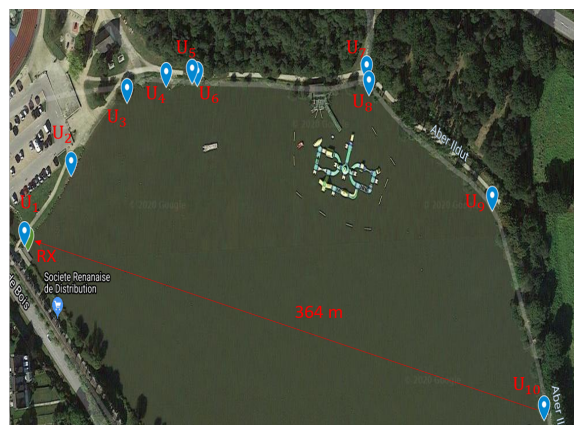


Figure 9. Experiment scheme on the Ty-Colo lake of St-Renan.

293 5.2. Watermark replay channel

294 To simulate a real experiment, we consider in this section the Watermark channel [17] which is
 295 a replay channel simulator driven by measurements of the time-varying CIR. The principle of the
 296 simulator consists of distorting input waveforms by convolving them with measured channels. To

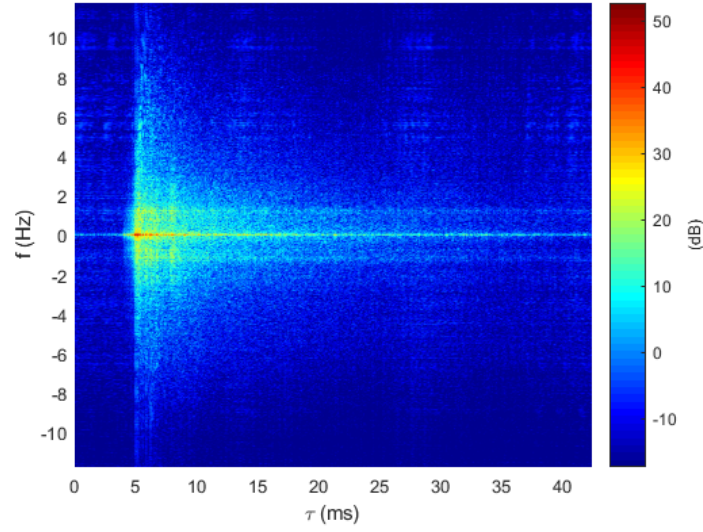


Figure 10. Delay-doppler spread function for the Ty-Colo lake.

297 simulate a multiuser communication, we sum the output of several Watermark channel fed by different
 298 CIRs and delayed by relative range of each user. The operation of channel replay for a static multiuser
 299 communication in the Single Input Single Output (SISO) case can be expressed in baseband as:

$$r(t) = \sum_{i=1}^{N_u} \int_{-\infty}^{+\infty} \hat{h}_i(\tau, t) s_i(t - \tau - \bar{\tau}_i) d\tau + n(t) \quad (25)$$

300 where $s_i(t)$ is the input signal, $\hat{h}_i(\tau, t)$ is the recorded CIR of the i -th user, $\bar{\tau}_i$ is communication delay
 301 between the i -th user and the receiver and $n(t)$ is a Gaussian noise.

302

303 For a mobile multiuser communication, the Doppler shift is simulated by resampling and
 304 phase-rotating the transmitted signal as follows:

$$r(t) = \sum_{i=1}^{N_u} \int_{-\infty}^{+\infty} \hat{h}_i(\tau, t) s_i((1 - a_i)(t - \tau - \bar{\tau}_i)) e^{j2\pi f_c a_i(t - \tau)} d\tau + n(t) \quad (26)$$

305 In the following, the Doppler shift will be known by the receiver and compensated by the relation (A1).
 306 Ty-Colo lake channels parameters are summarized in Table 3 whereas transmission system parameters
 307 are provided in Table 2.

Table 3. Watermark channel parameters.

Symbol	Signification	Value
f_c	Center frequency	27 kHz
f_s	Sampling frequency	96 kHz
B	Signal bandwidth	4 kHz
D_i	Transmission range	[47, 364] m
z_w	Water depth	5 m
SNR	Signal to noise ratio	10 dB
τ_{max}	RMS channel delay spread [20]	[4.31, 7.27] ms
σ_{max}	RMS channel Doppler spread [20]	[0.86, 2.51] Hz

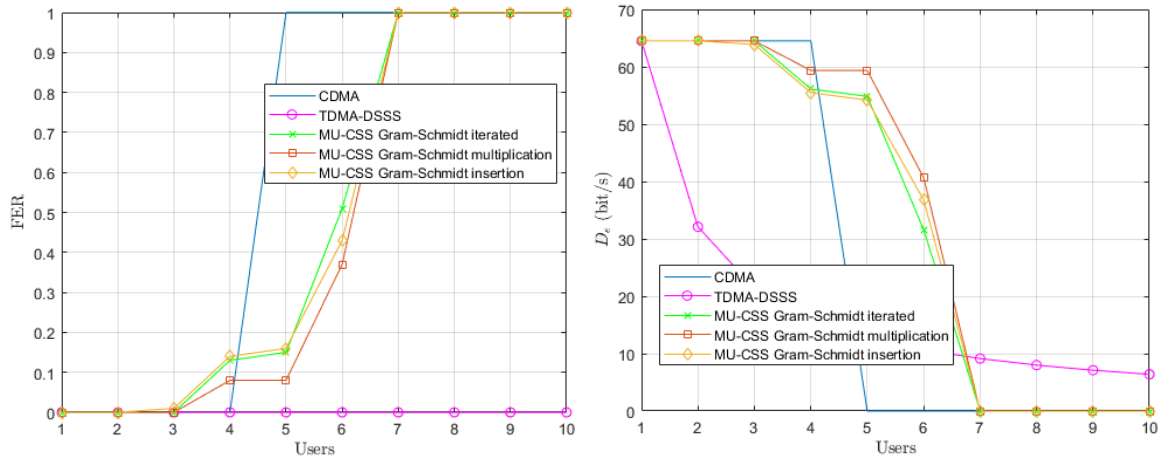


Figure 11. Average FER performance (left) and effective data rate per user (right) versus number of users for the Ty-Colo lake replayed channel with static users.

308 5.3. Performance results

309 5.3.1. Static users

310 Fig. 11 provides performance of multiuser transmission techniques over the Watermark channel
 311 fed by the Ty-Colo lake channel soundings. It can be noticed that the FER, and consequently the
 312 effective data rates, are worse than in simulation. This can be mainly explained by the fact the
 313 experimental soundings are very shallow water (≈ 5 m) leading to much more important multipath
 314 effect and, as consequence, to higher multiple access interference terms. Meanwhile, FER performance
 315 of MU-CSS transmissions are still better than CDMA ones up to 6 simultaneous users (except the
 316 case $N_u = 4$ where the CDMA is slightly ahead). Beyond this threshold, TDMA transmission is more
 317 suitable despite its low data rate due to a large number of users.

318 5.3.2. Mobile users

319 In Fig. 12, AUVs motion is emulated by adding motion-induced Doppler scale at the output of
 320 Watermark channel. For each frame, speed value of each AUV is randomly selected in the interval
 321 $[-2, 2]$ m/s. We can see that the performance of all access schemes are degraded excepted TDMA.
 322 From 1 up to 6 users, the MU-CSS transmissions remain globally more interesting in term of effective
 323 data rate. As seen in simulation, the MU-CSS with Gram-Schmidt insertion method is confirmed in
 324 experiments to provide highest robustness among all MU-CSS construction methods. Beyond 6 users,
 325 the TDMA is demonstrated to be more advantageous.

326 6. Conclusion and future works

327 In this paper, we have proposed a new multiuser transmission technique based on HFM
 328 signal denoted MU-CSS in the context of UWA communication within an AUVs fleet. By using the
 329 Gram-Schmidt orthogonalization, we derived three construction methods for MU-CSS allowing a
 330 very simple matched filter decoding scheme at the receiver side. Simulation comparisons against
 331 traditional CDMA with single user decoding over static and time-varying shallow water UWA models
 332 demonstrate a superior effective data rate for the proposed MU-CSS scheme even if the number
 333 of users is large and even if users are in motion, as for an AUV fleet. Experimental results with
 334 Watermark channel replay fed by channel soundings confirm the superiority of MU-CSS transmissions
 335 in a realistic scenario. The MU-CSS is demonstrated to be globally superior to CDMA up to 6 users.
 336 Beyond, the traditional TDMA approach is demonstrated to be more efficient. The MU-CSS approach

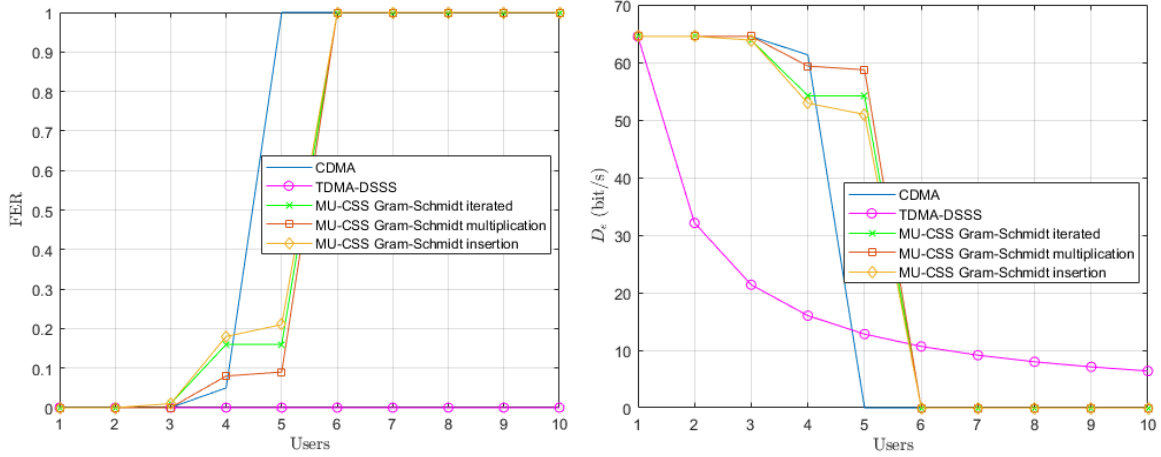


Figure 12. Average FER performance versus number of users for the Ty-Colo lake replayed channel with mobile users (left) and average effective data rate per user versus number of users for the Ty-Colo lake replayed channel with mobile users (right).

337 and especially associated with the Gram-Schmidt construction method offers a set of waveforms
 338 providing good orthogonal properties even in UWA uplink channel, so that such waveforms does
 339 not require complex multiuser decoding scheme at the receiver side. Thereby, MU-CSS transmission
 340 techniques constitute an interesting alternative to asynchronous CDMA for UWA network.

341

342 In a future work, we will consider multi-channel decoding for MU-CSS in order to improve the
 343 number of users to be correctly decoded simultaneously, and also taking into account real Doppler-shift
 344 estimation and impact to decoding performance when AUVs have different speeds and directions.

345 **Funding:** This research was partly funded by Thales DMS France in the framework of the WAVES laboratory. The
 346 APC was funded by L@bISEN Yncréa Ouest.

347 **Author Contributions:** Software, C. Bernard; writing—original draft preparation, C. Bernard and P.-J. Bouvet;
 348 writing—review and editing, A. Pottier and P. Forjonel.

349 **Conflicts of Interest:** The authors declare no conflict of interest.

350 Appendix. Calculation of $\gamma_{i,k}$, $\eta_{i,k}$ and $w_{i,k}$

351 The receive baseband signal after Doppler pre-processing can be expressed as:

$$z_i(t) = r \left(\frac{t}{1-a_i} \right) e^{-j2\pi f_c \left(\frac{a_i}{1-a_i} \right) t} \quad (\text{A1})$$

$$= \left(\sum_{j=1}^{N_u} \int_{-\infty}^{+\infty} h_j \left(\tau, \frac{t}{1-a_i} \right) s_j \left((1-a_j) \left(\frac{t}{1-a_i} - \tau \right) \right) e^{j2\pi f_c a_j \left(\frac{t}{1-a_i} - \tau \right)} d\tau \right) e^{-j2\pi f_c \left(\frac{a_i}{1-a_i} \right) t} \quad (\text{A2})$$

$$+ n \left(\frac{t}{1-a_i} \right) e^{-j2\pi f_c \left(\frac{a_i}{1-a_i} \right) t} \quad (\text{A3})$$

352 Combination of (2) and (7) yields:

$$\gamma_{i,k} = \int_{-\frac{T_s}{2}}^{\frac{T_s}{2}} \int_{-\infty}^{+\infty} h_i \left(\tau, \frac{t+kT_s}{1-a_i} \right) g_i^*(t) g_i(t - (1-a_i)\tau) e^{-j2\pi f_c a_i \tau} d\tau dt \quad (\text{A4})$$

$$\eta_{i,k} = \sum_{\substack{n=1 \\ n \neq k}}^{N_s} d_{i,n} \int_{-\frac{T_s}{2}}^{\frac{T_s}{2}} \int_{-\infty}^{+\infty} h_i \left(\tau, \frac{t + kT_s}{1 - a_i} \right) g_i^*(t) g_i(t - \tau - (n - k)T_s) e^{-j2\pi f_c a_i \tau} d\tau dt \quad (\text{A5})$$

$$+ \sum_{\substack{j=1 \\ j \neq i}}^{N_u} \sum_{n=1}^{N_s} d_{j,n} \int_{-\frac{T_s}{2}}^{\frac{T_s}{2}} \int_{-\infty}^{+\infty} h_j \left(\tau, \frac{t + kT_s}{1 - a_i} \right) g_i^*(t) g_j \left((1 - a_j) \left(\frac{t + kT_s}{1 - a_i} - \tau \right) - nT_s \right) e^{-j2\pi f_c \left(\frac{a_i - a_j}{1 - a_i} (kT_s + t) + a_j \tau \right)} d\tau dt \quad (\text{A6})$$

$$(\text{A7})$$

353 and

$$w_{i,k} = e^{-j2\pi f_c \frac{a_i}{1 - a_i} kT_s} \left(\int_{-\frac{T_s}{2}}^{\frac{T_s}{2}} g_i^*(t) n \left(\frac{t + kT_s}{1 - a_i} \right) e^{-j2\pi f_c \left(\frac{a_i}{1 - a_i} \right) t} dt \right) \quad (\text{A8})$$

354 Appendix. Justification of the MU-CSS Gram-Schmidt construction process

355 To have the orthogonality between the different $e_i(t)$, we use a variant of the Gram-Schmidt
 356 process [25], which is a method for orthogonalizing a set of vectors in an inner product space. The
 357 inner product is defined by $\forall f, g \in L^2(\mathbb{R})$ as $\langle f(t), g(t) \rangle = \int_{-\frac{T_s}{2}}^{\frac{T_s}{2}} f(t) g^*(t) dt$. Let $\{c_1(t), c_2(t)\}$ a set
 358 of linearly independent vectors. We add the vector $e_0(t)$ to the previous family and we build an
 359 orthogonal family from vector $e_0(t)$. By the Gram-Schmidt process, we have:

$$e_1(t) = c_1(t) + \alpha_1 e_0(t) \quad (\text{A9})$$

360 Using orthogonality, the previous equation gives:

$$\langle c_1(t), e_0(t) \rangle + \alpha_1 \|e_0(t)\|_2^2 = 0 \quad (\text{A10})$$

$$\Leftrightarrow \alpha_1 = - \frac{\langle c_1(t), e_0(t) \rangle}{\|e_0(t)\|_2^2} = - \frac{\int_{-\frac{T_s}{2}}^{\frac{T_s}{2}} c_1(t) e_0^*(t) dt}{\|e_0(t)\|_2^2} \quad (\text{A11})$$

361 For the last vector, the Gram-Schmidt process gives:

$$e_2(t) = c_2(t) + \beta e_0(t) + \alpha_2 e_1(t) \quad (\text{A12})$$

362 We take $\beta = 0$ because that is enough to have orthogonality and we obtain:

$$e_2(t) = c_2(t) + \alpha_2 e_1(t) \quad (\text{A13})$$

363 Using orthogonality, the previous equation becomes:

$$\langle c_2(t), e_1(t) \rangle + \alpha_2 \|e_1(t)\|_2^2 = 0 \quad (\text{A14})$$

$$\Leftrightarrow \alpha_2 = - \frac{\langle c_2(t), e_1(t) \rangle}{\|e_1(t)\|_2^2} = - \frac{\int_{-\frac{T_s}{2}}^{\frac{T_s}{2}} c_2(t) e_1^*(t) dt}{\|e_1(t)\|_2^2} \quad (\text{A15})$$

364 By generalization, we deduce the equation (10).

365 **References**

- 366 1. Stojanovic, M. Underwater Acoustic Communications: Design Considerations on the Physical Layer. 2008 Fifth Annual Conference on Wireless on Demand Network Systems and Services, 2008, pp. 1–10.
367 doi:10.1109/WONS.2008.4459349.
- 368 2. Stojanovic, M.; Beaujean, P.P.J. Acoustic Communication. In *Springer Handbook of Ocean*
369 *Engineering*; Dhanak, M.R.; Xiros, N.I., Eds.; Springer International Publishing, 2016; pp. 359–386.
370 doi:10.1007/978-3-319-16649-0_15.
- 371 3. Champion, B.T.; Joordens, M.A. Underwater swarm robotics review. *2015 10th System of Systems Engineering*
372 *Conference (SoSE) 2015*, pp. 111–116. doi:10.1109/SYBOSE.2015.7151953.
- 373 4. Abramson, N. Development of the ALOHANET. *IEEE Transactions on Information Theory* **1985**, *31*, 119–123.
374 doi:10.1109/TIT.1985.1057021.
- 375 5. Chirdchoo, N.; Soh, W.S.; Chua, K.C. Aloha-Based MAC Protocols with Collision Avoidance for
376 Underwater Acoustic Networks. *IEEE INFOCOM 2007 - 26th IEEE International Conference on Computer*
377 *Communications, 2007*, pp. 2271–2275. doi:10.1109/INFCOM.2007.263.
- 378 6. Colvin, A. CSMA with collision avoidance. *Computer Communications* **1983**, *6*, 227–235.
379 doi:10.1016/0140-3664(83)90084-1.
- 380 7. Otnes, R.; Asterjadhi, A.; Casari, P.; Goetz, M.; Husøy, T.; Nissen, I.; Rimstad, K.; Walree, P.v.; Zorzi,
381 M. *Underwater Acoustic Networking Techniques*; SpringerBriefs in Electrical and Computer Engineering,
382 Springer-Verlag: Berlin Heidelberg, 2012.
- 383 8. Trivedi, V.K.; Kumar, P. Carrier Interferometry Coded Single Carrier FDMA (CI/SC-FDMA) for Next
384 Generation Underwater Acoustic Communication. *Wireless Personal Communications* **2017**, *95*, 4747–4762.
385 doi:10.1007/s11277-017-4119-1.
- 386 9. Pompili, D.; Melodia, T.; Akyildiz, I.F. A CDMA-based Medium Access Control for UnderWater
387 Acoustic Sensor Networks. *IEEE Transactions on Wireless Communications* **2009**, *8*, 1899–1909.
388 doi:10.1109/TWC.2009.080195.
- 389 10. Konstantakos, D.; Tsimenidis, C.; Adams, A.; Sharif, B. Comparison of DS-CDMA and MC-CDMA
390 techniques for dual-dispersive fading acoustic communication networks. *IEE Proceedings - Communications*
391 **2005**, *152*, 1031–1038. Conference Name: IEE Proceedings - Communications, doi:10.1049/ip-com:20041152.
- 392 11. Stojanovic, M.; Freitag, L. Multichannel Detection for Wideband Underwater Acoustic CDMA
393 Communications. *IEEE Journal of Oceanic Engineering* **2006**, *31*, 685–695. doi:10.1109/JOE.2006.880389.
- 394 12. Yang, T.C. Spatially Multiplexed CDMA Multiuser Underwater Acoustic Communications. *IEEE Journal of*
395 *Oceanic Engineering* **2016**, *41*, 217–231. doi:10.1109/JOE.2015.2412993.
- 396 13. Yuan, F.; Wei, Q.; Cheng, E. Multiuser chirp modulation for underwater acoustic channel based on VTRM.
397 *International Journal of Naval Architecture and Ocean Engineering* **2016**, *9*. doi:10.1016/j.ijnaoe.2016.09.004.
- 398 14. Bernard, C.; Bouvet, P.J. Multiuser Underwater Acoustic Communication for an AUV Fleet. *OCEANS*
399 *2019 MTS/IEEE*, 2019.
- 400 15. Qarabaqi, P.; Stojanovic, M. Statistical Characterization and Computationally Efficient Modeling of a Class
401 of Underwater Acoustic Communication Channels. *IEEE Journal of Oceanic Engineering* **2013**, *38*, 701–717.
402 doi:10.1109/JOE.2013.2278787.
- 403 16. Aval, Y.M.; Wilson, S.K.; Stojanovic, M. On the Achievable Rate of a Class of Acoustic Channels and
404 Practical Power Allocation Strategies for OFDM Systems. *IEEE Journal of Oceanic Engineering* **2015**,
405 *40*, 785–795. doi:10.1109/JOE.2015.2451251.
- 406 17. Van Walree, P.; Socheleau, F.X.; Otnes, R.; Jensrud, T. The Watermark Benchmark for Underwater
407 Acoustic Modulation Schemes. *IEEE Journal of Oceanic Engineering* **2017**, *42*, 1007 – 1018.
408 doi:10.1109/JOE.2017.2699078.
- 409 18. Aval, Y.M.; Stojanovic, M. Differentially Coherent Multichannel Detection of Acoustic OFDM Signals. *IEEE*
410 *Journal of Oceanic Engineering* **2015**, *40*, 251–268. doi:10.1109/JOE.2014.2328411.
- 411 19. Aval, Y.M.; Wilson, S.K.; Stojanovic, M. On the Average Achievable Rate of QPSK and DQPSK OFDM Over
412 Rapidly Fading Channels. *IEEE Access* **2018**, *6*, 23659–23667. doi:10.1109/ACCESS.2018.2828788.
- 413 20. Proakis, J.G.; Salehi, M. *Digital Communications 5ed*, 5th edition ed.; McGraw-Hill: Boston, Mass., 2008.
- 414 21. R.L. Peterson, R.Z.; Borth, D. *Introduction to spread-spectrum communications*; Prentice Hall, 1995.
- 415

- 416 22. Zhou, S.; Wang, Z. *OFDM for Underwater Acoustic Communications*; John Wiley & Sons, Ltd: Chichester, UK,
417 2014. doi:10.1002/9781118693865.
- 418 23. Kebkal, K.G.; Bannasch, R. Sweep-spread carrier for underwater communication over acoustic channels
419 with strong multipath propagation. *The Journal of the Acoustical Society of America* **2002**, *112*, 2043–2052.
- 420 24. Kaminsky, E. Chirp signaling offers modulation scheme for underwater communications. *SPIE Newsroom*
421 **2006**. doi:10.1117/2.1200608.0357.
- 422 25. S.Lang. *Introduction to Linear Algebra*; Springer-Verlag New York Inc., 1985.
- 423 26. Sharif, B.S.; Neasham, J.; Hinton, O.R.; Adams, A.E. A computationally efficient Doppler compensation
424 system for underwater acoustic communications. *IEEE Journal of Oceanic Engineering* **2000**, *25*, 52–61.
425 doi:10.1109/48.820736.
- 426 27. van Walree, P. Channel Sounding for Acoustic Communications: Techniques and Shallow-Water Examples.
427 *Norwegian Defence Research Establishment (FFI), Tech. Rep. FFI-rapport* **2011**, *7*.

428 © 2020 by the authors. Submitted to *Sensors* for possible open access publication under the terms and conditions
429 of the Creative Commons Attribution (CC BY) license (<http://creativecommons.org/licenses/by/4.0/>).